Establishment of a Serum Tumor Marker for Preclinical Trials of Mouse Prostate Cancer Models

Isaac Van Huizen,[1,2] Guojun Wu,[1] Madeleine Moussa,[2] Joseph L. Chin,[1] Aaron Fenster,[3] James C. Lacefield,[3] Hideki Sakai,[4] Norman M. Greenberg,[5] and Jim W. Xuan[1,2]

Abstract Current prostate cancer research in both basic and preclinical trial studies employ genetically engineered mouse models. However, unlike in human prostate cancer patients, rodents have no counterpart of prostatic-specific antigen (PSA) for monitoring prostate cancer initiation and progression. In this study, we established a mouse serum tumor marker from a mouse homologue of human prostate secretory protein of 94 amino acids (PSP94). Immunohistochemistry studies on different histologic grades from both transgenic and knock-in mouse prostate cancer models showed the down-regulation of tissue PSP94 expression ($P < 0.001$), the same as for PSA and PSP94 in humans. The presence of mouse serum PSP94 was shown by affinity column and immunoprecipitation purification using a polyclonal mouse PSP94 antibody. A competitive ELISA protocol was established to quantify serum PSP94 levels with a sensitivity of 1 ng/mL. Quantified serum levels of mouse PSP94 ranged from 49.84 ng/mL in wild-type mice to 113.86, 400.45, and 930.90 ng/mL in mouse prostatic intraepithelial neoplasia with microinvasion, well differentiated, moderately differentiated, and poorly differentiated prostate cancer genetically engineered prostate cancer mice, respectively ($P < 0.01$, $n = 68$). This increase in serum PSP94 is also well correlated with age and tumor weight. Through longitudinal monitoring of serum PSP94 levels of castrated mice (androgen ablation therapy), we found a correlation between responsiveness/refractory prostate tissues and serum PSP94 levels. The utility of mouse serum PSP94 as a marker in hormone therapy was further confirmed by three-dimensional ultrasound imaging. The establishment of the first rodent prostate cancer serum biomarker will greatly facilitate both basic and preclinical research on human prostate cancer.

Prostate cancer remains the most frequently diagnosed malignancy among North American males and is second only to lung cancer in mortality (1). Genetics, diet, and lifestyle are just some of the factors that contribute to the development of prostate cancer (2). PSA is the only prostate cancer marker widely used for population screening, diagnosis, and monitoring of prostate cancer. The use of PSA as a serum marker has increased our ability to detect prostate cancer, select therapy, and to monitor outcomes (3–5).

Authors' Affiliations: Departments of [1]Surgery, [2]Pathology and [3]Imaging Research Laboratories, Robarts Research Institute, University of Western Ontario, London, Ontario, Canada; [4]Department of Urology, Nagasaki University School of Medicine, Nagasaki, Japan; and [5]Clinical Research Division, Fred Hutchinson Cancer Research Center, Seattle, Washington

Received 5/2/05; revised 6/27/05; accepted 7/5/05.

Grant support: Canadian Institute of Health Research grants UOP-63722 and MT-15390, NIH-National Cancer Institute grant 2 U01 CA084296-06, Prostate Cancer Research Foundation of Canada, Canada Foundation for Innovation and the Ontario Innovation Trust Canada Research Chair funds (A. Fenster), and CIHR University-Industry Scientist salary award (J.W. Xuan).

The costs of publication of this article were defrayed in part by the payment of page charges. This article must therefore be hereby marked *advertisement* in accordance with 18 U.S.C. Section 1734 solely to indicate this fact.

Requests for reprints: Jim W. Xuan, Urology Research Laboratory, London Health Sciences Centre, 375 South Street, London, Ontario, N6A 4G5, Canada. Phone: 519-667-6682; Fax: 519-432-7367; E-mail: jim.xuan@lhsc.on.ca.

doi:10.1158/1078-0432.CCR-05-0953

Prostate cancer has proven to be a complicated disease due to its heterogeneous and multifocal nature (6, 7). Consequently, much research has been devoted to elucidating the mechanisms of the disease. This has led to the construction of genetically engineered mouse models of prostate cancer using transgenic and knock-out techniques that attempt to model the human clinical situation in all aspects (for reviews, see refs. 6, 8). Rat probasin gene-based transgenic adenocarcinoma prostate (TRAMP; ref. 9) and LPB-SV40 tag (LADY; ref. 10) models are currently the most prevalent murine prostate cancer models.

Unlike in humans, murine models of prostate cancer currently lack established biomarkers for the disease, specifically serum biomarkers (review refs. 6, 7). A serum marker is an affordable noninvasive screening test that can monitor treatment efficacy and disease recurrence disease-free state. The ability to noninvasively quantify tumor burden in living conditional tumor model mice will ultimately lead to the development of more accurate models of human cancer that are better suited to evaluating and optimizing preclinical cancer therapy.

Because mice do not produce and express a human PSA analogous, the search begins for other equals in mice. Prostatic secretory protein of 94 amino acids (PSP94), also known as β-microseminoprotein (11–15), is one of the three most abundantly secreted proteins (0.5-1 mg/mL in semen) from the prostate gland (the others being PSA and prostatic acid phosphatase). Both PSA and PSP94 can leak out from the

prostate glandular ducts into the blood circulation at a detectable concentration (3, 4, 14, 15). The abnormal protein levels in serum in prostate cancer patients indicate irregular or erratic control of the secretion of prostate cancer cells and possibly defective or less efficient tissue barrier (3–5, 16, 17). The similar tissue distribution of PSA and PSP94 in secretory tissues and their similar means of escape from prostate secretory ducts into the general circulation suggest a similar control mechanism of secretion of these two proteins (3, 4, 14, 15). PSP94 expression in prostate tissue has been shown as having a statistical correlation with histologic grade (13, 18–21). This association is inversely correlated (that is, as tumor grade advances PSP94 expression decreases), the same as in PSA (3, 4, 16, 17). As with PSA, much research has investigated the use of PSP94 as a prostate cancer marker in humans in terms of serum bound free forms, urine levels, and tissue expression (14, 15).

To investigate the use of mouse PSP94 as a serum biomarker for mouse prostate cancer model studies, we did a study to show, detect, and quantify PSP94 in the mouse serum.

Materials and Methods

Expression and purification of polyhistidine containing recombinant mouse PSP94. A cDNA fragment coding for the mature form of mouse PSP94 (22) was amplified and inserted into the polyhistidine containing vector (pTrcHis A, Invitrogen, Carlsbad, CA) as reported previously (23). An *Escherichia coli* strain DH5α (Invitrogen) was used to purify large amounts of recombinant protein (23), following the manufacturer's recommendations. Matrix-assisted laser desorption ionization and electrospray ionization tandem mass spectrometry protein sequencing was used for the identification of pTrcHis-Mouse PSP94. For sequencing, 10 μg of recombinant protein were run on 15% SDS-PAGE, the band was excised from the gel, and in-gel trypsin digestion was done.

Generation of rabbit antiserum against recombinant fusion proteins of pTrcHis-mPSP94. Rabbit polyclonal antibodies against pTrcHis mouse PSP94 proteins were obtained using a standard procedure (SOP #370-01, University of Western Ontario Animal Care Committee). In brief, ~2.5 mg of recombinant mouse PSP94 (1.0 mL) was emulsified in 1.0 mL of Freund's adjuvant (incomplete, from Sigma, St. Louis, MO) and injected i.m. into rabbits 1 kg in size. A second booster (1.5 mg) injection was done 2 weeks later.

Genetically engineered mouse prostate cancer models. In previous studies, we used a 3.84-kb promoter enhancer region of the *PSP94* gene to target the expression of the SV40T/t antigen oncogene specifically to the mouse prostate [strain F1 (C57BL 6 × CBA)] to establish a genetically engineered prostate cancer model called PSP94-transgenic mouse of adenocarcinoma in the prostate (PSP-TGMAP; refs. 18, 24). Similar to the TRAMP model, PSP-TGMAP mice developed fast-growing tumors specifically in the prostate within 4 to 8 months of age. In view of limitations of transgenic technique-derived prostate cancer models, we established a knock-in mouse adenocarcinoma prostate model (PSP-KIMAP) by targeting the SV40 Tag at the *PSP94* gene, which showed close-to-human prostate cancer features (19, 20).

Mouse blood collection, animal handling and dissection, and tissue lysate preparation. Mice were anesthetized at a dose of 0.03 mL/10 g of a ketamine xylazine mixture (anesthesia stock: 100 mg/mL ketamine and 20 mg/mL xylazine). Tail blood sample collection to a maximum volume of 300 μL at any one time from living mice was conducted with light anesthesia following the published protocols (25). Blood was removed via the tail every 2 to 3 weeks (25). When maximum blood samples were required, collection was through the chest cavity with deep anesthesia.

Mouse prostate tissue dissection was done as previously reported (18–20, 26). Tissue samples from the prostate and the male accessory gland were freshly dissected and homogenized in a lysis buffer: 1% SDS, 1 mmol/L phenylmethylsulfonyl fluoride, and 0.01 mol/L PBS. For histologic studies, tissues were fixed in 10% formalin (Fisher, Ottawa, Ontario, Canada) and embedded in paraffin. Orchidectomy (castration) operations were done through scrotum access. All animal experiments were conducted according to protocols approved by the University Council on Animal Care.

Histologic grading, immunohistochemistry, and immunostaining evaluation. Histologic grading was done according to the Mouse Models for Human Consortium Committee Prostate Pathology Committee Bar Harbour Classification System (27). Histopathologic characterization and standard definitions of various degrees of mouse prostatic intraepithelial neoplasia (mPIN), well-differentiated, moderately differentiated, and poorly differentiated prostate cancers, were classified as previously reported (18–20).

For immunohistochemistry analyses, formalin-fixed, paraffin-embedded, 4.0-μm sections were stained as previously reported (18, 19, 28). Each immunohistochemistry staining specimen was assessed independently by three authors (I.V.H., G.W., and M.M) and a consensus of grading was reached. The intensity of the staining was graded on a scale of 0 to ≥2 indicating no staining, weak, and strong staining respectively as previously reported (21). The extent of the staining in tumor foci was classified as 0%, 1% to 25%, 26% to 50%, 51% to 75%, and 76% to 100% as previously reported (21, 29). Antibodies used in this study were high titer rabbit antiserum against pTrcHis mPSP94 and androgen receptor (AR, Affinity Bioreagents, Golden, CO). Dilution factors used were 1:5,000 and 1:250, respectively.

Preparation of affinity column using antiserum of mouse PSP94, immunoprecipitation, and Western blotting. pTrcHis mPSP94 antiserum was coupled to a 1-mL HiTrap NHS–activated Sepharose High Performance column (Amersham Biosciences, Montreal, Quebec, Canada) in a standard coupling buffer [0.2 mol/L $NaHCO_3$, 0.5 mol/L NaCl (pH 8.3)] for 30 minutes at room temperature. All uncoupled active groups were deactivated via alternating washes of Buffer A [0.5 mol/L ethanolamine, 0.5 mol/L NaCl (pH 8.3)] and Buffer B [0.1 mol/L acetate, 0.5 mol/L NaCl (pH 4)]. The column was then equilibrated with a neutral buffer [binding buffer: 50 mmol/L Tris, 0.15 mol/L NaCl (pH 7)]. All samples tested were equilibrated with the binding buffer and passed through the column overnight at 4°C at a flow rate of 1 mL/min. The column was then washed with binding buffer and eluted [elution buffer: 100 mmol/L glycine, 150 mmol/L NaCl, 1% Triton (pH 3)]. The purified sample was then desalted using a HiTrap Desalting column (Amersham Biosciences).

Immunoprecipitation was done using Rabbit IgG TrueBlot (eBioscience, San Diego, CA). Roughly 5 μg of pTrcHis mPSP94 polyclonal antibody was incubated with each sample and then added to 50 μL of anti-rabbit immunoglobulin IP beads. The beads were then washed with sample buffer [50 mmol/L Tris-HCl (pH 8.0), 150 nmol/L NaCl, 1% NP40], boiled with an SDS loading buffer for 3 minutes, and loaded onto a 15% SDS-PAGE gel for Western blotting.

For Western blotting experiments, an enhanced chemiluminescent kit (Amersham) was used and an horseradish peroxidase–conjugated anti-rabbit IgG (rabbit IgG TrueBlot, eBioscience) was used as a secondary antibody.

Glycosylation detection of mouse PSP94 was done using a commercial kit (Glyco-Pro, Sigma). Deglycosylation was done using a commercial kit (Glyko, Prozyme, San Leandro, CA) and the denaturing protocol was followed.

Establishment of a competitive ELISA protocol for quantification of serum PSP94. Levels of serum PSP94 were quantified by a competitive ELISA as previously reported (30–33). For all assays, recombinant pTrcHis mPSP94 was used as the coating antigen (100 ng per well); 96-well immunoplates (Nunc, Life Technologies, Mississauga, Ontario, Canada) were coated at 4°C overnight in coating buffer [1.4 mmol/L Na_2CO_3, 7 mmol/L $NaHCO_3$ (pH 9.2)]. The coated plate was washed thrice in PBS (phosphate-buffered saline) and blocked in 1.5% bovine serum albumin (RIA grade, Sigma) in PBS-T at 37°C for 1 hour. PSP94

antiserum was diluted 1:40,000 in 1.5% bovine serum albumin/PBS with *E. coli* (isomerase block) lysate and preincubated for 1 hour. Blocked antiserum was then added to standards/samples and incubated for 1.5 hours. Competitor mixtures were then added to immunoplates and incubated for 30 minutes. Horseradish peroxidase–conjugated goat antiserum anti-rabbit IgG was diluted (1:1,000) and incubated for 1 hour. The plate was then washed and incubated in 0.4 mg/mL *o*-phenylene diamine dihydrochloride (Sigma) and 0.05% H_2O_2 in developing buffer [35 mmol/L citric acid, 67 mmol/L Na_2HPO_4 (pH 5.0)] for 20 minutes. Standard curves were plotted by relative absorbency (B/B_0) against competitor standard protein (ng/mL). Relative absorbency (B/B_0) was calculated as follows: $B = A_{595\ nm}$ of the sample − nonspecific binding (NSB). NSB was determined by testing $A_{595\ nm}$ with excess standard (1 μg) in the competition reaction to entirely block the antibody (i.e., under maximum competition and minimum antibody binding to the plate). $B_0 = A_{595\ nm}$ of the maximum antibody binding (no competition) − NSB.

Levels of serum PSP94 quantification. Various mouse serum samples (50 μL per well) were run in triplicate as described above, and protein concentrations were interpolated from the logarithmic equation for the corresponding trend line [e.g., $y = -0.3364\ln(x) + 0.3429$]. Mice were grouped according to tumor grade and age (19, 20). Eleven- to 24-week-old KIMAP mice were characterized as PIN with microinvasion; 20- to 52-week-old mice were characterized as well-differentiated prostate cancer and 32- to 91-week-old mice as moderately differentiated and poorly differentiated prostate cancer.

Three-dimensional ultrasound image acquisition. We followed the protocols as reported elsewhere (24). Ultrasound images were acquired using a commercial microimaging system (Vevo 660, VisualSonics, Inc., Toronto, Ontario, Canada). Three-dimensional image acquisition and reconstruction required ~30 seconds. The sagittal diameters of the tumors were measured using the electronic calipers of the three-dimensional ultrasound display software.

Statistical analysis. All statistical analyses were done by statistical software packages of SPSS (version 10.0) and SigmaPlot 2000 (SPSS Scientific, Chicago, IL), with consultations from a statistician, including preparation of linear diameter growth curves, χ^2 and ANOVA analyses, etc.

Results

Characterization of a polyclonal antibody against recombinant pTrcHis mPSP94. We have previously reported the production of several kinds of antibodies for mouse PSP94 studies, all of which lacked high titer and specificity (23). As shown in SDS-PAGE (Fig. 1A), according to the standard protocol using the heavy metal affinity column provided by the manufacturer, two dominant protein bands were always copurified at an apparent molecular weight of 20.8 and 15 kDa separately. Matrix-assisted laser desorption ionization and electrospray ionization tandem mass spectrometry sequencing was done on these two purified proteins, which were identified as isomerase and pTrcHis mPSP94, respectively, and both contained several histidine rich areas (data not shown). Considering that mouse PSP94 is a small-sized peptide (93 amino acids, 10.6 kDa) of weaker antigenecity, we used the larger bacteria band (peptidyl-prolyl *cis/trans*-isomerase from *E. coli*, 20.8 kDa) as a carrier protein, which should act the same as other glutathione *S*-transferase fusion proteins we used (23), to elicit a stronger immune response. A higher dose of antigen (2.5 mg pTrcHis mPSP94/rabbit) was used to obtain polyclonal rabbit antiserum. Western blotting analysis showed the antibody to be both sensitive and specific (Fig. 1A and B) for isomerase and pTrcHis mPSP94.

Western blot analysis was also conducted on natural mouse PSP94 from the ventral prostate lysate and found to be very specific (Figs. 1E and 3B). Because the antibody detected a wide band with smearing, a kit was used to detect glycosylation of PSP94 (Fig. 1C). A broad range of glycosylated mouse PSP94 proteins, shown as positive magenta bands, were observed (Fig. 1C), indicating the protein is heavily glycosylated (pTrcHis mPSP94 was used as a negative control). As a control, human PSP94 protein (10 μg) purified from human semen (30) was loaded for a comparison. Figure 1D shows

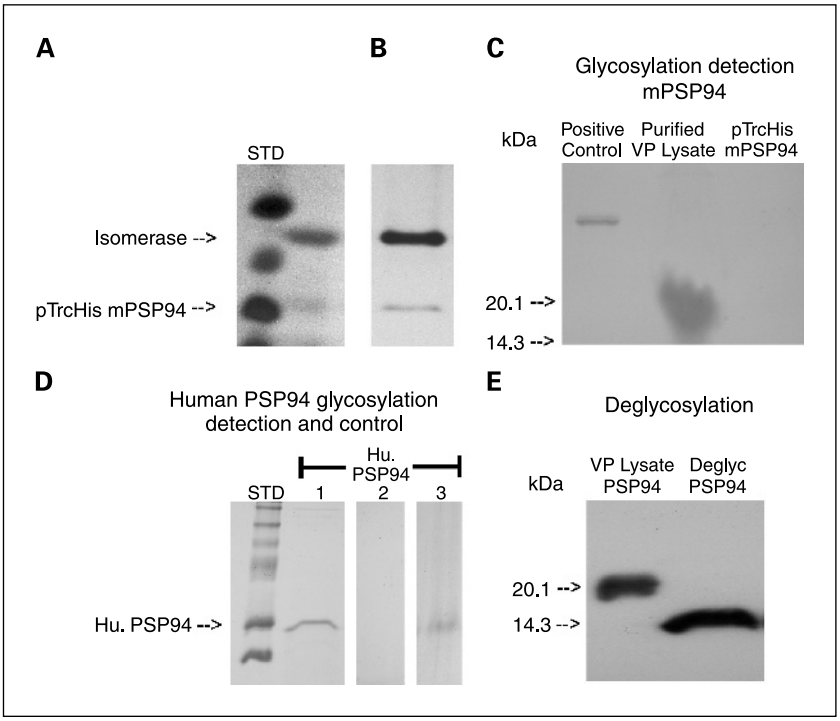

Fig. 1. Mouse prostate tissue PSP94 is glycosylated as demonstrated by a polyclonal antibody against recombinant pTrcHis mouse PSP94. SDS-PAGE and Coomassie blue staining (*A*) and Western blotting (*B*) analyses of the purified recombinant pTrcHis mPSP94 (bottom band). Recombinant mouse PSP94 is shown at apparent molecular weight of ~15 kDa. *C,* demonstration of glycosylation of mouse prostate tissue (ventral prostate, *VP*) PSP94 protein. All samples were purified using a polyclonal mouse PSP94 antibody (see Materials and Methods and Fig. 2). Magenta staining indicates protein glycosylation is positive. The positive glycosylation control protein (horseradish peroxidase, *left*) was provided by the kit (see Materials and Methods). Ten micrograms of pTrcHis mPSP94 (*right*) and purified human (*Hu*) seminal PSP94 (26, 27) were loaded as negative controls. *D,* SDS-PAGE showing the purified human seminal PSP94 (5, 10 μg each lane), loaded as a comparison for glycosylation tests. Lane 1, positive human PSP94 control. Lane 2, glycosylation detection of human PSP94. Lane 3, Commassie staining of lane 2 gel. *E,* Western blotting showing the deglycosylation test of mouse prostate PSP94 in the prostate tissue lysate (10 μg per lane loaded from a lysate of 100 mg wet weight/mL). Prestained standard protein ladder (Invitrogen) used are (from bottom) 8.4, 14.9, 19.6, 26, 37.4 kDa.

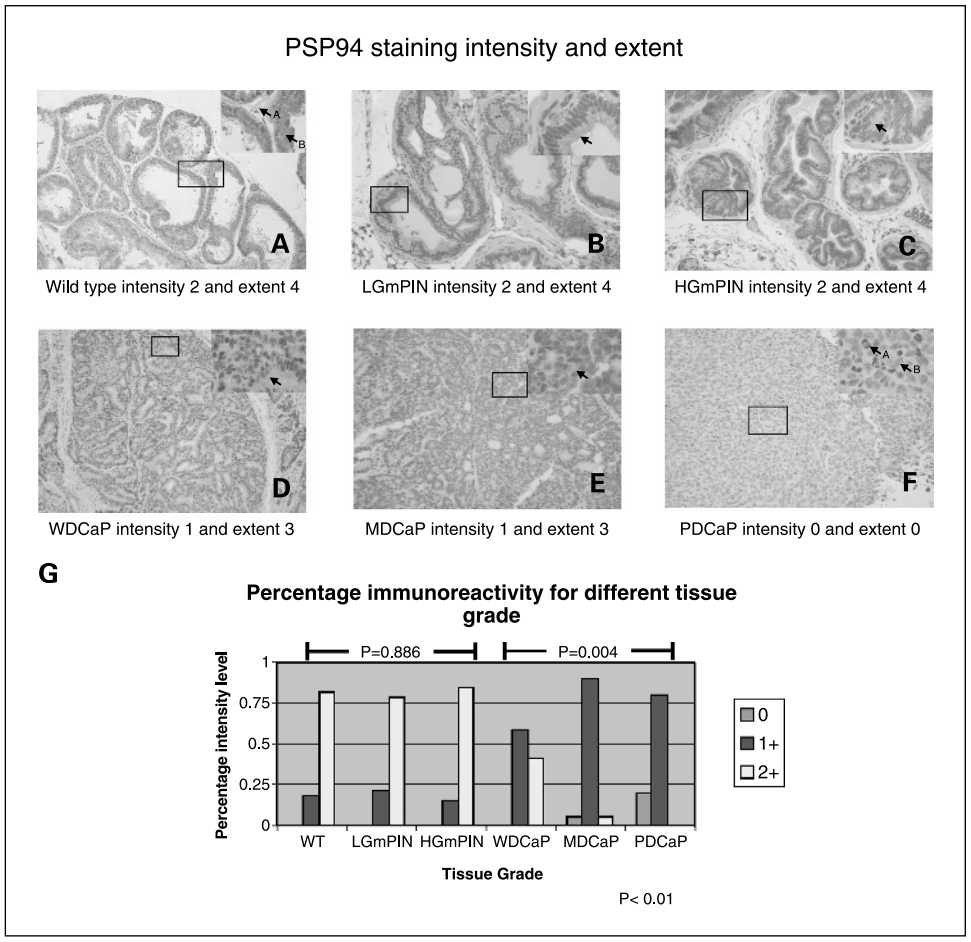

Fig. 2. Histologic analysis of prostate tissue PSP94 expression from genetically engineered prostate cancer mouse models. *A*, strong PSP94 expression (≥2) in wild-type prostate tissue with a 76% to 100% extent of staining (20×). *A*, highlighting the stain free stroma (*inset*, 40×). *B*, strong PSP94 expression (≥2) in low-grade mPIN prostate tissue with a 76% to 100% extent of staining (20×). Inset, stained cytoplasm of the secretory cells where PSP94 is located (40×). *C*, strong PSP94 expression (≥2) in high-grade mPIN area with an extent of 76% to 100% (20×). Arrow points to the stained cytoplasm of the secretory cells (40×). *D*, moderate intensity of PSP94 staining (≥1) in well-differentiated prostate cancer with an extent of 51% to 75% (20×). At higher magnification (40×), nuclear atypia is clear as well as staining localization of PSP94 to the cytoplasm of the secretory cells. *E*, moderate intensity of PSP94 staining (≥1) in moderately differentiated prostate cancer with an extent of 51% to 75% (20×). Inset, boxed area of nuclear atypia and proliferating cells with weaker staining localized in the cytoplasm of the secretory cells (*arrow*). *F*, negative PSP94 expression (0) in poorly differentiated prostate cancer with higher magnification revealing nuclear atypia (*arrow B*) and cell proliferation (*arrow A*). *G*, plot of the correlation of immunoreactivity with prostate cancer progression. Abbreviations: WT, normal wild-type mice; LGmPIN, low-grade mouse PIN; HGmPIN, high-grade mouse PIN; WDCaP, well-differentiated prostate cancer; MDCaP, moderately differentiated prostate cancer; PDCaP, poorly differentiated prostate cancer. Difference between grade and immunoreactivity is significant ($P < 0.001$).

a Coomassie blue SDS-PAGE staining of the purified human PSP94 protein. Glycosylation detection for human seminal PSP94 (Fig. 1D) was negative. Deglycosylation reaction was done to confirm the glycosylation of mouse PSP94 from prostate tissue lysates. Western blots (Fig. 1E) showed a stronger band with lower molecular weight (14.3 kb) after deglycosylation, probably due to focusing of the deglycosylated PSP94 protein.

Down-regulation of the prostate tissue PSP94 expression is associated with different tumor grades as shown by immunohistochemistry. The antibody for pTrcHis mPSP94 was further characterized via immunohistochemistry staining and found to be specific for the cytoplasm of the epithelial cells of the prostate gland (Fig. 2). No stromal staining was detected. PSP94 expression was tested in 100 different tissue fixed blocks from adult mice of different tumor grade [i.e., wild type (n = 11), low-grade mPIN (n = 19), high-grade mPIN (n = 23), well-differentiated (n = 22), moderately differentiated (n = 18), and poorly differentiated (n = 15) prostate cancer] and genetically engineered lines (TGMAP and KIMAP). Strong positive staining intensity (≥2) was found primarily in normal glandular tissue, low-grade mPIN, and high-grade mPIN foci. Strong positive staining, however, could also be found in well-differentiated and moderately differentiated prostate cancer with a decreasing incidence, respectively (Fig. 2). Conversely, poorly differentiated, moderately differentiated, and well-differentiated prostate cancers had a higher incidence of weak and negative staining (≥1 and 0). χ^2 tests revealed a significant difference in the intensity between all grades ($P < 0.01$) as well as in the intensity of prostate cancer tissues only ($P_2 = 0.004$). There was, however, no significant difference in the intensity of wild type, low-grade mPIN, and high-grade mPIN tissues ($P_1 = 0.886$). These data suggest that PSP94 expression decreases as prostate cancer progresses, possibly due to the "leaking out" of PSP94 into the surrounding vasculature. The extent of staining was also noted among the different tissues (data not shown) and was significantly different between all grades ($P = 0.003$). However, no significant difference in staining extent was noted among the non-prostate cancer tissues and the prostate cancer tissues ($P_1 = 0.145$ and $P_2 = 0.062$).

Demonstration of the presence of mouse PSP94 in the serum of wild-type mice by affinity column separation and purification. Next, we intend to test, as for PSA and PSP94 in humans, whether mPSP94 is able to "leak" into the mouse vasculature. To show the presence of mouse PSP94 in serum, an affinity column using the polyclonal PSP94 antibody described above was established. The column was then used to purify recombinant pTrcHis mPSP94 to show column activity. Figure 3A shows that recombinant protein was purified with a high yield and little to no protein was lost in the pass and wash. Because equivalent amounts of samples were loaded in the gel, the addition of each elution represents the final column yield. Next, PSP94 from mouse ventral prostate lysates was passed through the column to determine if the column could purify

natural mouse PSP94 (Fig. 3B). The column successfully purified mouse PSP94 with a yield of roughly 40%. Little to no mouse PSP94 was observed in the column pass; however, a substantial amount was noted in the first column wash. Finally, 2 and 4 mL of wild-type mouse serum were passed through the column, and mouse PSP94 was eluted (Fig. 3C). Column passes and washes yielded no mouse PSP94 but did have some nonspecific protein, most likely due to the high protein content of serum. Ventral prostate lysate mouse PSP94 band was used as a positive control and was found to match up with serum elutions. Furthermore, increasing amounts of mouse PSP94 were noted for larger sample sizes of serum.

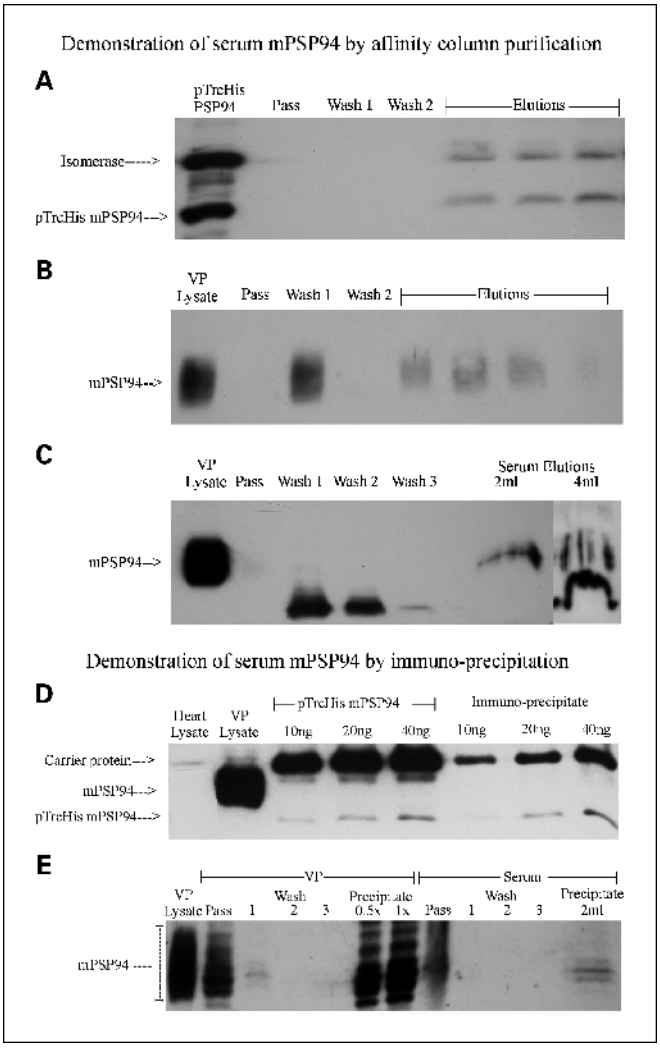

Fig. 3. Western blots of the presence of mouse serum PSP94 via affinity column and immunoprecipitation techniques. All samples, including recombinant pTrcHis mPSP94 and natural mouse PSP94 from ventral prostate (*VP*) tissue lysate and serum in blots (*A*) to (*C*), were purified using the affinity column. Ventral prostate lysate – positive controls were loaded from a 100 mg/mL standardized sample. *A*, Western blots of pTrcHis mPSP94 by Affinity column. *B*, Western blots showing purification of the lysate of natural mouse PSP94 from ventral prostate tissue by affinity column. *C*, Western blot showing the presence of mouse PSP94 in the serum of wild-type mice (2- and 4-mL serum samples used). The irregular bands observed for the different serum elutions are most likely due to high salt concentrations despite samples being desalted. For immunoprecipitation experiments (*D* and *E*), all samples were precipitated using the same polyclonal mouse PSP94 antibody used for the affinity column. Ventral prostate lysate – positive controls were loaded from a 100 mg/mL standardized sample. *D*, Western blot showing that the immunoprecipitation technique works properly with the recombinant pTrcHis mPSP94 with a good yield. *E*, Western blots showing that the precipitation technique works for natural mouse PSP94 and also detects the presence of mouse PSP94 in the serum of wild-type mice (2-mL serum used). Equivalent and comparable samples were loaded for each Western blot.

Further demonstration of the existence of PSP94 in mouse serum was by immunoprecipitation experiments. The same logical steps were taken as in affinity column, producing the same results (Fig. 3). First, recombinant pTrcHis mPSP94 was precipitated to show the technique was working properly (Fig. 3D). Second, natural mouse PSP94 was precipitated from ventral prostate lysate (Fig. 3E). Like in affinity column, substantial amounts of mouse PSP94 washed off in the pass and first wash; however, a significant amount was visible in the precipitate. In the same blot, 2 mL of serum were precipitated. Due to the high protein content of serum, the pass had significant nonspecific background. No mouse PSP94 was detected in the subsequent washes and the precipitate revealed a multiband mouse PSP94. The multiple bands observed for immunoprecipitation and not Affinity column purification may be due to the fact that in immunoprecipitation the antibody is free in solution and may bind to PSP94 differently. Glycosylation of mPSP94 may also play a role in this phenomenon. Both affinity column and immunoprecipitation produced comparable amounts of mouse PSP94 precipitate for 2 mL of serum.

Establishment of competitive ELISA standard curves using recombinant pTrcHis mouse PSP94 as coating antigen. To show that mouse serum PSP94 is quantifiable, two sets of immunoassays were done for obtaining standard curves that will quantify serum mouse PSP94 levels and show the assay is functional for natural mouse PSP94. The first standard graph used recombinant pTrcHis mPSP94 as both the coating antigen and the competitor (Fig. 4A). This assay consistently produced a linear logarithmic graph with a negative slope, indicating the assay was working. The next step was to confirm the sensitivity of the assay applied to natural mouse PSP94. Figure 4B is an example of the resultant standard curve when using recombinant pTrcHis mPSP94 as the coating antigen, and mouse PSP94 from the ventral prostate lysate as the competitor. This standard graph produced no slope and showed the assay could not distinguish between different levels of mouse PSP94. It was thought that because the carrier protein isomerase most likely produced the most antibodies in our polyclonal antibody, it was overpowering our immunoassay. This was not noticed in our standard graph using recombinant pTrcHis mPSP94 as the competitor because, in that case, isomerase coated to the plate had competition. Consequently, *E. coli* lysate containing isomerase was used to block our polyclonal antibody and remove any signal produced by isomerase competition. Two new standard curves (Fig. 4C and D) were generated using this technique. Again, using pTrcHis as the competitor, the assay produced a linear graph with a negative slope (Fig. 4C). The same results were obtained when using the ventral prostate lysate (natural mouse PSP94) as the competitor, indicating the assay was functional for detecting mouse PSP94 (Fig. 4D). This new assay using *E. coli* lysate to block out isomerase activity was consequently used to quantify mouse PSP94 in our unknown serum samples.

Quantification of mouse PSP94 in serum from mice of different age groups via established competitive ELISA techniques. From the established standard graph technique (Fig. 4C), serum

mouse PSP94 levels were quantified (Fig. 4E). In our system, 50 μL of serum separated from mouse tail blood were assayed by ELISA for each well. Average serum levels for wild-type mice were 49.84 ng/mL. Average serum levels for KIMAP mice with mPIN with microinvasion, well-differentiated prostate cancer, and moderately/poorly differentiated prostate cancer were 113.86, 400.45, and 930.90 ng/mL, respectively (Fig. 4E). Compared with wild-type mice, serum PSP94 levels increase significantly ($P < 0.001$, ANOVA) with both tumor grade and age in KIMAP mice. This increase is synchronous to increases of grades from well- to moderately differentiated prostate cancer in our KIMAP model (19, 20). No significant difference was noted between wild type and mPIN with microinvasion ($P = 0.941$).

Next, to correlate serum PSP94 levels with tumor weight, a correlation of tumor weight and age in KIMAP was established (Fig. 4F). No detectable differences were observed before the age of 33 weeks (Fig. 4F). Larger error bar for 72- to 91-week-old mice was found reflecting nonsynchronous tumor growth in the late stage of KIMAP mice as previously reported (19, 20). Comparing Fig. 4E and F, it was found that serum PSP94 levels increased the most when average tumor weight increased significantly (from age of 20-35 to 35-91 weeks). Correlation of tumor weight with serum PSP94 was shown from wild type, mPIN with microinvasion, well-differentiated prostate cancer, and most of moderately differentiated prostate cancer (Fig. 4E).

Demonstration of use of serum PSP94 marker to monitor hormone therapy (castration) in genetically engineered prostate cancer mouse models. To show use of serum PSP94 in preclinical trial studies, PSP94 levels were tested for their responsiveness and refractory to androgen deprivation therapy in our transgenic (PSP-TGAMP) and knock-in (PSP-KIMAP) mouse prostate cancer models.

Castration was used for mimicking hormone therapy in two groups of mice with prostate cancer. The first group was used to test for tumors in well- and moderately differentiated prostate cancer development (not at the late stage of prostate cancer development with massive metastasis) in our recently established knock-in prostate cancer (PSP-KIMAP) model (19, 20). Five PSP-KIMAP mice at the age of 10 months were subjected to orchidectomy operation. Tail blood samples were collected before castration and 2 and 5 weeks after castration. As shown in Fig. 5A, there was a significant decrease in serum PSP94 levels ($P < 0.001$) after castration. Histologic analysis of prostate tissue showed significant involution as a result of the androgen deprivation (Fig. 5B and C). Immunohistochemistry analysis for

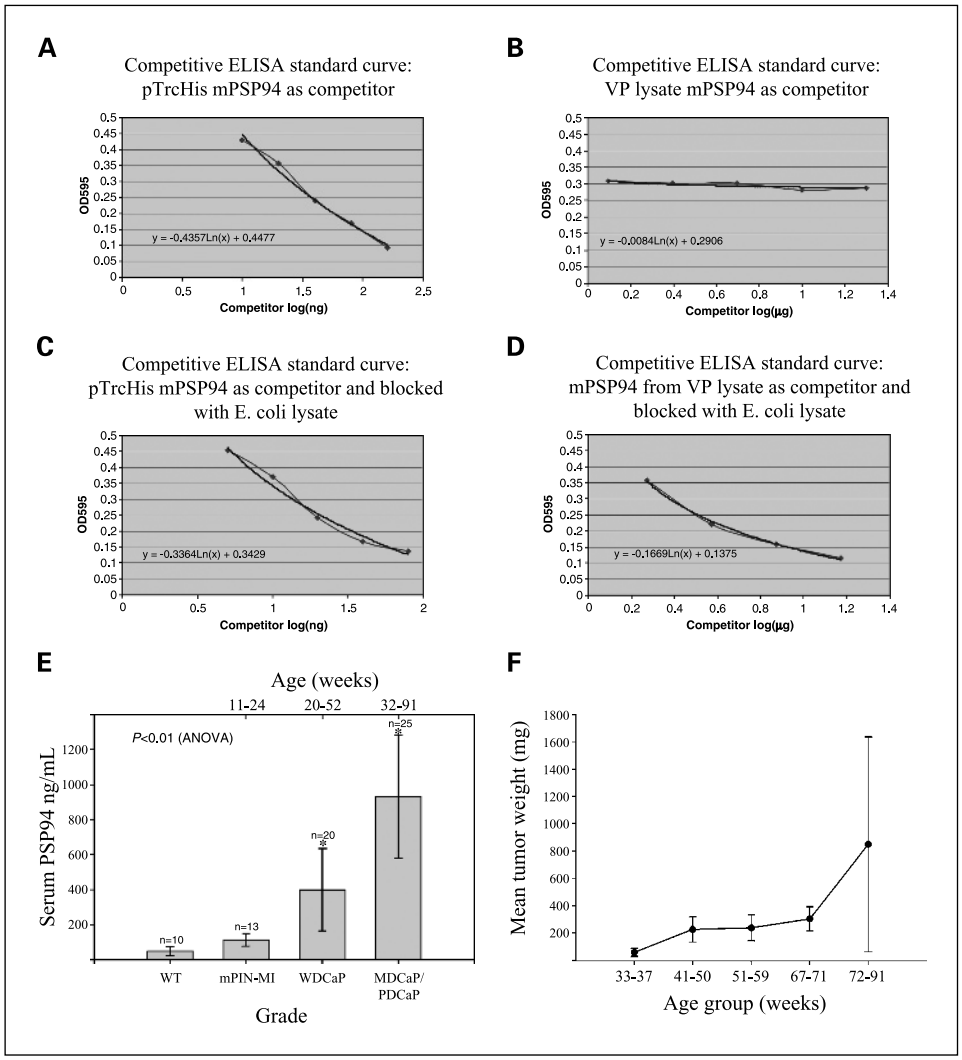

Fig. 4. Establishment of standard curves for quantifying levels of serum PSP94 by a competitive ELISA protocol and quantification of average serum mouse PSP94 levels for KIMAP mice from different tumor grades and age groups matched with average tumor weight. *A*, standard competitive ELISA curve with pTrcHis mPSP94 protein as competitor. *B*, standard competitive ELISA curve with natural mouse PSP94 from ventral prostate tissue lysate as competitor (*VP lysate* = 100 μg/μL). *C*, similar competitive ELISA as in (*A*), but polyclonal mouse PSP94 antibody was competed (blocked) with *E. coli* cell (DH5α) lysate to remove the dominant antibodies for carrier protein isomerase. This type of standard competitive ELISA curve was used for quantifying levels of mouse serum PSP94. *D*, according to standard curve of (*C*), one example of the competitive ELISA assays ability to detect natural mouse PSP94 in ventral prostate lysates (by log[μg]). Logarithmic line (*in bold*) of the best fit (MS Excel) used to interpolate unknown PSP94 levels from serum samples. *E*, sixty-eight serum levels from various KIMAP mice were calculated via interpolation from a standard graph (e.g., *C*) of known levels of recombinant pTrcHis mPSP94. Mice were grouped according to tumor grade (*bottom*) and age (*top*). Bars, SD. *, $P < 0.01$ compared with wild-type mouse PSP94 levels ($P < 0.01$, ANOVA). *F*, graph of prostate cancer (ventral prostate and DLP) weight of KIMAP mice plotted against age groups, showing a steady prostate cancer growth of prostate cancer in KIMAP model in 1 year and heterogeneity of tumor growth in late stage (after 1 year). Prostate tumor weight was indicated by mean ± SD mg/mouse: 58 ± 29.7 mg (27-39 weeks, $n = 12$), 224.9 ± 91.6 mg (40-52 weeks, $n = 9$), 236.8 ± 94.0 mg (53-65 weeks, $n = 7$), 260 ± 89.3 mg (67-71 weeks, $n = 16$), and 850 ± 1520 mg (72-91 weeks, $n = 6$). The later stage (>70 weeks) error bar was out of the range and only half value was shown.

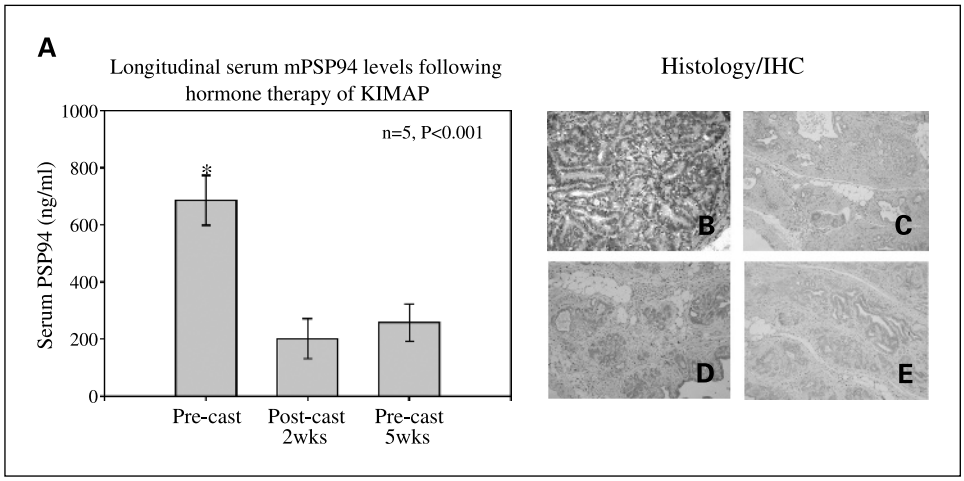

Fig. 5. Serum mPSP94 levels before and after androgen deprivation therapy for KIMAP mice ($n = 5$) along with histologic analysis. *A,* serum mPSP94 levels (ng) before and after castration showing a significant reduction in response to therapy ($P = 0.001$). *B-E,* histologic analysis of prostate demonstrating involution of gland structure and altered PSP94 and AR expression (10×). *B* and *C,* H&E staining of tissue samples from KIMAP mouse prostate before and after castration, respectively. Increased stroma to gland ratio is evident in (*C*). *D,* AR expression after castration. *E,* PSP94 expression after castration.

AR and PSP94 showed a reduction in expression compared with noncastrated mice (Fig. 2B, D, and E). Because AR staining was still present (Fig. 5D), the observed PSP94 expression may be attributed to testosterone secreted from the adrenal gland.

To test for refractory of hormone therapy in preclinical trials, genetically engineered prostate cancer mice at later stages of prostate cancer with large tumor mass were selected for hormone therapy (castration). Only PSP-TGMAP mice were selected. A new method developed in our laboratory for acquisition and analysis of three-dimensional ultrasound images of mouse prostate cancer models (24) was employed to assist the diagnosis by PSP94 serum marker. This is because of the following considerations: (a) PSP-TGMAP mice revealed exuberant tumor growth with neuroendocrine features (as did the TRAMP and LADY models), which the genetically engineered prostate cancer tumor mass could reach extraordinary sizes of up to 15 g/35 body weight in just 2 weeks time (19, 20, 24). (b) Our University Council on Animal Care protocols mandate a 2-week time interval limit for collecting tail blood and more frequent collection is not possible. (3) It is important to assess the effectiveness of the serum marker. A total of three mice were castrated and two were imaged.

Figure 6A illustrates that serum levels of PSP94 in castrated mice decreased 2 weeks after castration and then stabilized at a higher level than normal wild-type mice. This may indicate the incomplete responsiveness of prostate cancer after castration. Furthermore, longitudinal three-dimensional ultrasound imaging of a castrated mouse in Fig. 6B revealed that the tumor decreased slightly in size from 4.37 to 3.97 mm in diameter (Fig. 6B, *row 1*) 1 week after castration. Continual tumor expansion was observed in three-dimensional imaging (*rows 2-3*) from 1 to 7 weeks after castration. Based on the longitudinal imaging data and measurements of tumor diameters, a tumor growth curve was established (Fig. 6C), along with noncastrated mice ($n = 3$) as a control. The growth curve shows that castration (hormone therapy) in mice with late stages of prostate cancer slowed and delayed the rapid tumor growth rate and increased survivability. Responsiveness to castration (hormone therapy) was brief (first week after castration), which is consistent with the results from the serum PSP94 tests (Fig. 6A). Histologic analysis (Fig. 6D) also showed that in castrated mice, even in poorly differentiated prostate cancer tissues, atrophy is evident, which is the reason for increased survivability (Fig. 6C). Immunohistochemistry experiments with several prostate cancer marker genes (*AR* and *PSP94*) were done to further show that the androgen therapy was, in fact, working. The expression levels for each of the two markers used were decreased when compared with the levels of genetically engineered prostate cancer mice with the same cancer grade (Fig. 6D).

Discussion

PSA as the "gold standard" for the early detection and tracking of tumor progression has revolutionized the management of prostate cancer (3, 4). Rising PSA levels after prostatectomy or radiotherapy generally predicts clinical recurrence. In contrast to the number of markers developed for human prostate cancer, rodents have few tumor markers and no identified PSA counterpart (gene or protein). A prostate-specific serum tumor marker as effective as or more effective than PSA would greatly assist in longitudinal observations of prostate cancer development in genetically engineered prostate cancer models in both basic and preclinical trial studies. By exploring PSP94 as a serum marker for mouse prostate cancer models, we will contribute uniquely to the establishment of a preclinical trial model for prostate cancer.

In contrast to PSA showing no counterpart in rodent species, PSP94 has analogous proteins in humans, primates, pigs, and rodents. These studies have shown that PSP94 is a conserved but also a rapidly evolving, protein (minireview; refs. 22, 26). We have previously shown that, at the transcriptional and protein expression levels, rodent PSP94 expression is strictly prostate tissue specific (26, 34). We have also found serum bound forms of PSP94 (14, 15), similar to serum-bound forms of PSA (35, 36). PSA and PSP94 may thus have a similar application as serum markers for prostate cancer.

Before establishing mPSP94 as a serum biomarker in mice, we failed in constructing an antibody against mouse natural PSP94 with high specificity and immunoreactivity (23). In this study, we have discovered that, unlike human PSP94, mouse PSP94 is glycosylated. This may suggest that glycosylation of mouse PSP94 protein contributes an important role as an immunogen. Glycosylation of mPSP94 may play a role in the reduced affinity of our recombinant antibody to natural mouse PSP94 by blocking epitope structures of mouse PSP94. This

observation is further supported by the fact that our antibody has a significantly higher affinity for our recombinant pTrcHis protein, which is not glycosylated (Fig. 1). This reduction in affinity caused problems when establishing standard curves for quantifying mouse serum PSP94 (Fig. 4) and must be addressed to refine the immunoassay.

We have shown that PSP94 is present in mouse serum by both affinity column and immunoprecipitation methods. Through the established competitive ELISA technique in this study, we have also shown that the concentration of mouse serum PSP94 levels is higher than human PSA levels, although the range (ng/mL) for human PSA and PSP94 is similar.

The use of mouse PSP94 as a serum marker lies in its ability to distinguish between mice with or without prostate cancer even before the tumor is palpable. In this study, mice with genetically engineered prostate cancer from both transgenic and knock-in mouse models were investigated. Both models represent two types of tumor developmental kinetics, fast and protract (18–20, 24). At a tissue level, we showed that mouse PSP94 protein expression decreases as prostate cancer progresses in a statistically significant way (Fig. 2G). This decrease correlated with tumor intensity, rather than the extent of the tumor staining (Fig. 2), indicating that intensity is the leading factor for determining the rate at which PSP94 may leak into the surrounding vasculature. Through ELISA techniques, we showed that PSP94 increased with tumor grade and age in our KIMAP model of prostate cancer indicating that PSP94 serum levels were affected by cancer grade ($P < 0.01$, ANOVA). Furthermore, significant elevation of serum PSP94 was found to correlate with significant increases in average tumor weight in a majority of our KIMAP mice (19, 20).

An important issue for preclinical trials is to test the responsiveness and refractory of prostate cancer to hormone therapy. We have shown the use of a serum marker in monitoring preclinical trials for hormone therapy of genetically engineered prostate cancer mice in our newly established PSP-KIMAP model, with the majority of well- and moderately differentiated prostate cancer.

By doing castration experiments, we have shown that serum PSP94 could be used as an indicator for the responsiveness of hormone therapy. We have also tested refractory to hormone therapy in PSP-TGMAP mice with a later stage of prostate cancer development. In the PSP-TGMAP model, as with in the TRAMP model, transgenic mice reveal rapid and exuberant

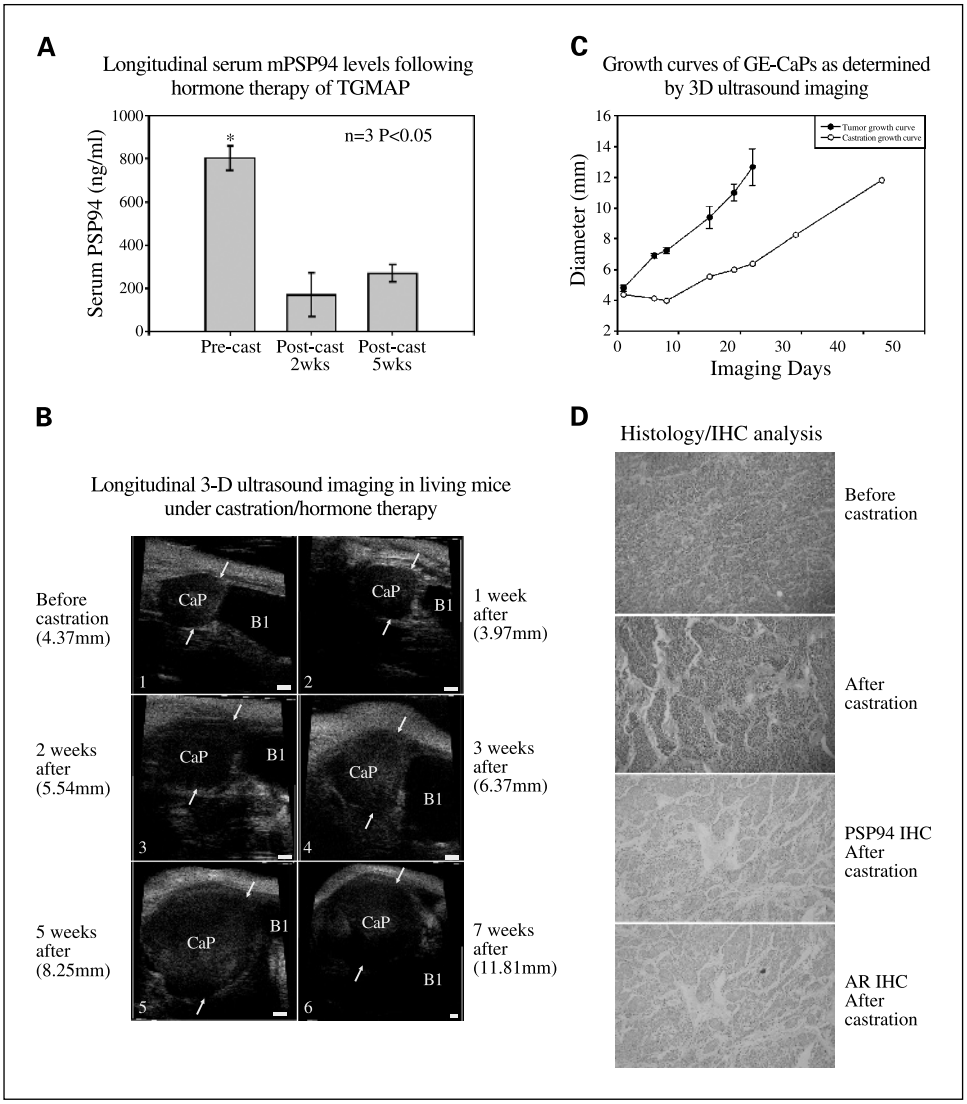

Fig. 6. Combined tests of mouse serum PSP94 levels and three-dimensional (*3-D*) ultrasound imaging before and after androgen deprivation therapy (castration) for TGMAP mice at late stage of genetically engineered prostate cancer (*GE-CaP*) development. *A*, serum mPSP94 levels (ng) before and after castration showing a significant reduction in response to therapy followed by refractory ($n = 3$, $P < 0.05$). *B*, longitudinal detection by three-dimensional ultrasound imaging in living castrated mice with rapid ventral prostate tumor development. 1-6, representative two-dimensional slices from six different three-dimensional ultrasound images before castration and at different time points after castration. 1, mouse was 21 weeks old when the tumor was first detected (measuring 4.37 mm in diameter) and was then castrated (day 1). 2-5, the same tumor on days 8, 15, 22, 29, and 43 as the tumor diameter went from 3.97 to 5.54, 6.37, 8.25, and 11.81 mm, respectively. Ventral surface of the abdominal wall (*top*) and deeper abdominal and retroperitoneal structures (*bottom*). Bar, 1 mm. Prostate (*CaP*) and bladder (*B1*) positions. *C*, determination of growth curve in PSP-TGMAP mice based on three-dimensional ultrasound imaging data of (*B*). Rapid tumor growth rate is shown in this graph for transgenic mice with genetically engineered prostate cancers. The control group was PSP-TGMAP mice ($n = 3$) without castration. The maximum sagittal diameter of the tumor was plotted against the day after initial observation/castration. *D*, histologic analysis of the castrated prostate tissues demonstrating involution of gland structure and altered PSP94 and AR expression (10×). Before castration was from the age matched, late stage of prostate cancer in TGMAP mice. Involution in the prostate tissue under castration was evident. Immunohistochemistry analysis of the prostate tissue showed weak PSP94 and AR expression in poorly differentiated prostate cancer.

prostate cancer growth with logarithmic volume expanding in a very short time (18–20, 24). Because of the speed of tumor growth and time constraints for mouse blood sampling, daily monitoring of serum levels will not be possible and thus other techniques must be used. We showed that three-dimensional ultrasound imaging could supplement the tumor biochemical marker for longitudinal observations in living conditions in the preclinical trial. The recently developed three-dimensional ultrasound imaging technology applied to genetically engineered prostate cancer mice in our laboratories has shown many advantages (24). By combining serum marker analysis and three-dimensional ultrasound imaging, we have developed a solid technique for monitoring prostate cancer longitudinally with consistent accuracy. Biochemical serum markers and biomedical imaging in living animals have great value for both basic and preclinical trial studies of prostate cancer.

Acknowledgments

We thank the UWO Transgenic and Gene Targeting Facility, VisualSonics, Inc. for in-kind and technical support, Canada Foundation for Innovation and the Ontario Innovation Trust for ultrasound microimaging system, and Michael Bygrave for assistance with ultrasound image acquisition.

References

1. Jemal A, Murray T, Samuel A, Ghafoor A, Ward E, Thun MJ. Cancer statistics, 2003. CA Cancer J Clin 2004;53:5–26.
2. Steiner MS, Gingrich JR. Gene therapy for prostate cancer: where are we now? J Urol 2000;164:1121–36.
3. Oesterling JE, Martin SK, Bergstralh EJ, Lowe FC. The use of prostate-specific antigen in staging patients with newly diagnosed prostate cancer. JAMA 1993;269:57–60.
4. Stamay TA, Yang N, Hay AR, McNeal JE, Freiha FS, Redwine E. Prostate-specific antigen as a serum marker for adenocarcinoma of the prostate. N Engl J Med 1987;317:909–16.
5. Therasse R, Aubuck S, Eisenhauer E. New guidelines to evaluate the response to treatment in solid tumors. J Natl Cancer Inst 2000;92:205–16.
6. Huss WJ, Maddison LA, Greenberg NM. Autochthonous mouse models for prostate cancer: past, present and future. Semin Cancer Biol 2000;11:245–60.
7. Winter SF, Cooper AB, Greenberg NM. Models of metastatic prostate cancer: a transgenic perspective. Prostate Cancer Prostatic Dis 2003;6:204–11.
8. Abate-Shen C, Shen MM. Mouse models of prostate carcinogenesis. Trends Genet 2002;18:S1–5.
9. Greenberg NM, Demayo F, Finegold MJ, et al. Prostate cancer in a transgenic mouse. Proc Natl Acad Sci U S A 1995;92:3439–43.
10. Masumori N, Thomas TZ, Chaurand P, et al. A probasin-large T antigen transgenic mouse line develops prostate adenocarcinoma and neuroendocrine carcinoma with metastatic potential. Cancer Res 2001;61:2239–49.
11. Hara M, Kimura H. Two prostate-specific antigens, γ-seminoprotein and b-microseminoprotein. J Lab Clin Med 1989;113:541–8.
12. Abrahamsson PA, Lilja H, Falkmer S, Wadstrom LB. Immunohistochemical distribution of the three predominant secretory proteins in the parenchyma of hyperplastic and neoplastic prostate glands. Prostate 1988;12:39–46.
13. Hyakutake H, Sakai H, Yogi Y, et al. β-Microseminoprotein immunoreactivity as a new prognostic indicator of prostatic carcinoma. Prostate 1993;22:347–55.
14. Wu D, Guo YZ, Chambers AF, Izawa JI, Chin JL, Xuan JW. Serum bound forms of PSP94 (prostate secretory protein of 94 amino acids) in prostate cancer patients. J Cell Biochem 1999;76:71–83.
15. Reeves JJ, Xuan JW, Arfanis K, et al. Identification, purification and characterization of a novel human blood protein with binding affinity for prostate secretory protein of 94 amino acids. Biochem J 2005;385:105–14.
16. Grande M, Carlstrom K, Rozell BL, Stege R, Pousette A. Prognostic value of serial tissue prostate-specific antigen measurements during different hormonal treatments in prostate cancer patients. Clin Cancer Res 2000;6:1790–5.
17. Stege R, Grande M, Carlstrom K, Tribukait B, Pousette A. Prognostic significance of tissue prostate-specific antigen in endocrine-treated prostate carcinomas. Clin Cancer Res 2000;6:160–5.
18. Gabril MY, Onita T, Ji PG, et al. Prostate targeting: PSP94 gene promoter/enhancer region directed prostate tissue-specific expression in a transgenic mouse prostate cancer model. Gene Ther 2002;9:1589–99.
19. Duan WM, Gabril MY, Moussa M, et al. Knock-in of SV40 Tag oncogene in a mouse adenocarcinoma of the prostate (KIMAP) model demonstrates advantageous features over the transgenic model. Oncogene 2005;24:1510–24.
20. Gabril MY, Duan WM, Wu GJ, et al. A novel knock-in prostate cancer model demonstrates biology similar to that of human prostate cancer and suitable for preclinical studies. Mol Ther 2005;11:348–62.
21. Imasato Y, Xuan JW, Sakai H, et al. PSP94 expression after androgen deprivation therapy: a comparative study with prostate specific antigen in benign prostate and prostate cancer. J Urol 2000;164:1819–24.
22. Xuan JW, Kwong J, Chan FL, et al. cDNA, genomic cloning and gene expression analysis of mouse PSP94 (prostate secretory protein of 94 amino acids). DNA Cell Biol 1999;18:11–26.
23. Thota A, Karajgikar M, Duan WM, et al. Mouse PSP94 expression is prostate tissue-specific as demonstrated by a comparison of multiple antibodies against recombinant proteins. J Cell Biochem 2003;88:999–1011.
24. Wirtzfeld LA, Wu GJ, Bygrave M, et al. Three-dimensional ultrasound micro-imaging for preclinical studies using a transgenic prostate cancer mouse model. Cancer Res 2005;65:6337–45.
25. Hoff J. Methods of blood collection in the mouse. Lab Anim 2000;29:47–53.
26. Imasato Y, Onita T, Moussa M, et al. Rodent PSP94 gene expression is more specific to the dorsolateral prostate and less sensitive to androgen ablation than probasin. Endocrinology 2001;142:2138–46.
27. Shappell SB, Thomas GV, Roberts RL, et al. Prostate pathology of genetically engineered mice: definitions and classification. The consensus report from the Bar Harbor meeting of the Mouse Models of Human Cancer Consortium Prostate Pathology Committee. Cancer Res 2004;64:2270–305.
28. Park JH, Walls JE, Galvez JJ, et al. Prostatic intraepithelial neoplasia in genetically engineered mice. Am J Pathol 2002;161:727–35.
29. Lazure C, Villemure M, Gauthier D, Naude RJ, Mbikay M. Characterization of ostrich (*Struthio camelus*) β-microseminoprotein (MSP): identification of homologous sequences in EST databases and analysis of their evolution during speciation. Protein Sci 2001;10:2207–18.
30. Xuan JW, Wu D, Guo Y, Fraser J, Chin J. Recombinant PSP94 (prostate secretory protein of 94 amino acids) demonstrates similar linear epitope structure as natural PSP94 protein. J Cell Biochem 1996;63:61–74.
31. Xuan JW, Wu D, Guo Y, Huang CL, Wright GL, Jr., Chin JL. Analysis of epitope structure of PSP94 (prostate secretory protein of 94 amino acids): (II) Epitope mapping by monoclonal antibodies. J Cell Biochem 1997;65:185–97.
32. Xuan JW, Wu D, Guo Y, Garde SV, Baijal-Gupta M, Chin JL. Analysis of epitope structure of PSP94 (prostate secretory protein of 94 amino acids): (I) immunodominant and immuno-recessive area. J Cell Biochem 1997;65:172–85.
33. Bauman GS, Xuan JW, Chin J, et al. PSP94: Evaluation of prognostic utility in patients treated with radiotherapy for nonmetastatic prostate cancer. Prostate 2000;2:94–101.
34. Kwong J, Xuan JW, Choi HL, Chan PSF, Chan FL. PSP94 (or b-microseminoprotein) is a secretory protein specifically expressed and synthesized in the lateral lobe of the rat prostate. Prostate 2000;42:219–29.
35. Lilja H, Christenssson A, Dahlen U, et al. Prostate-specific antigen in serum occurs predominantly in complex with a1-antichymotrypsin. Clin Chem 1991;37:1618–25.
36. Stenman U, Hakama M, Knekt P, Aromaa A, Teppo L, Leinonen J. Serum concentrations of prostate specific antigen and its complex with a1-antichymotrypsin before diagnosis of prostate cancer. Lancet 1994;344:1594–8.